Energetics analysis of polyethylene crystallization: single crystal growth surfaces

A. K. Patel and B. L. Farmer
Materials Science and Engineering, Washington State University, Pullman, Washington 99164, USA

Semiempirical energy calculations have been used to investigate the structure and energetics of molecular attachment and mobility on the {110} and {200} growth faces of polyethylene single crystals. The results indicate that, while the crystallographic position of the first nucleating segment on the {110} face is a low energy position, other dispositions of the molecule have somewhat lower energy. Growth layers nucleated by molecules in the lowest energy position are substantially different from the crystallographic structure. After inclusion of a few molecules however, this growth layer must undergo a rearrangement requiring the cooperative motions of several molecules in order to assume the now lower energy crystalline structure. Comparisons of the energies and mobility of molecular segments on the {110} and {200} growth faces indicate that there is a greater attraction of the segments to the {200} face, but that chain mobility is substantially greater on the {110} face. Correlation of these factors with the observed dependence of degree of truncation of polyethylene single crystals on crystallization temperature and the concentration of polymer in solution suggests that the nucleation energetics take precedence over factors of chain mobility, but the total truncation behaviour observed is probably the result of an interplay between these two factors. Energetics calculations also provide an explanation for the observed lower melting temperature of the {200} sectors.

INTRODUCTION

There have been many investigations to elucidate the nature of polymer crystals, particularly in two research areas. First, molecular structures of many crystalline materials have been described, as have the morphological structures wherein a molecular structure expresses itself at a sub-macroscopic level of aggregation. Such descriptions are largely based on direct experimental observation. Second, molecular growth mechanisms of these polymeric crystalline materials have been described more by inference and extrapolation, relying upon comparison between theoretical prediction and experimental observation for the evaluation of any particular description. Thus, crystallization mechanisms result in visible structures but do not have an experimental visibility of their own at the molecular level.

It is particularly important then that a variety of theoretical–predictive treatments be used to give as broad a base as possible to our understanding of the polymer crystallization mechanism. A technique of polymer research not yet used in investigations of the crystallization process *itself* is energetics analysis, which essentially involves computerized model building (the geometric specification of atomic or molecular positions) and evaluation (the summation of atomic interactions through the model system).

Energetics analysis has progressed from isolated chain, conformational calculations to the study of defects and molecular motions occurring in crystalline or a partially disordered environment. More recently the energetics and motions of conformational defects (crankshafts and kinks)[1–3] and the possible effects of structural defects (methyl branches) on the mechanical behaviour of a host crystal[4–7] have been studied. Various aspects of the regular structures formed by linear chains can also be investigated. Polyethylene offers advantages of relative structural simplicity and an atomic composition that can be satisfactorily analysed using available empirical energy functions[8]. The geometry and energetics of the association of a polyethylene chain segment on crystal growth faces and the energetics involved in the movement of such a chain on the growth face can be examined.

This investigation has been concerned with polyethylene single crystals as they are generally envisaged to grow from relatively dilute solution. The morphology and crystal structure of polyethylene crystals have been described quite extensively[9–15]. Of relevance here is that a diamond-shaped polyethylene single crystal has the *a* and *b* crystallographic axes lying parallel to the long and short diagonals of the crystal, respectively. The growth planes of the crystals are {110} faces. When the temperature of crystallization and/or the concentration of the polymer in solution is greater than some critical value (characteristic of the solvent used), the crystals become truncated in the *a* direction[16–18]. Truncation in the *a* direction occurs symmetrically, giving six sectors in the high-temperature crystal. The two new sectors possess {200} growth faces.

Theory of growth

Crystals formed by linear polymers are mostly molecular, i.e. the forces that hold the body of the crystal intact are of the van der Waals type[19]. Various treatments of the

0032–3861/80/020153–11$02.00

problem of lamellar thickness and growth have been given[20–29]: those yielding both growth rate and lamellar thickness data consistent with experimental observations are based on surface nucleation theory[20–23,25–27]. The one given here is after Lauritzen and Hoffman[22]. The polymer molecule is assumed to have a cross-sectional area ab, where a is the width of the molecule. A surface nucleus of fixed thickness b and height l (fixed at a specified undercooling) grows along the growth face. When ν stems and $\nu_f = \nu - 1$ folds have been formed, the free energy of formation (ignoring chain end effects) is

$$\Delta F_s = 2bl\sigma + 2\nu_f ab\sigma_e - \nu abl\Delta f \quad (1)$$

For large ν, this becomes

$$\Delta F_s = abl\sigma + \nu ab(2\sigma_e - l\Delta f) \quad (2)$$

where σ is the lateral surface free energy, σ_e the fold surface free energy and Δf is the free energy difference per unit volume between unbounded crystal and unbounded melt. The value of σ for polyethylene is in the range 10–15 ergs cm^{-2} (refs 31, 32). The fold surface free energy σ_e for polyethylene has been determined to be 93 ± 8 ergs cm^{-2}, (ref 19).

Growth of the crystal requires addition of new molecules to the growth faces. At various stages in this process a new fold plane must be nucleated on a completed growth face. Lauritzen and Hoffman[22] consider that the surface nucleus starts by a polymer segment (or set of segments) attaching itself to the crystal surface and coming into crystallographic register with the substrate, forming the first stem at a cost of $2bl\sigma$. The molecule then folds back on itself and continues to crystallize, largely in positions adjacent to the previous stem. The surface nucleus approaches and attains the region of stability (negative free energy) as it grows on the growth face. Many molecules can be involved in completing the surface strip and new molecules start to crystallize in the niche where the previous molecule terminated.

The surface nucleus has maximum free energy of formation at or near $\nu = 1$, and then gradually approaches the region of stability as ν increases. The change in free energy when the first step element is added to a completed growth face is

$$\Delta F_s(1) = bl(2\sigma - a\Delta f) \quad (3)$$

Since $2\sigma > a\Delta f$ in the temperature range of interest[33], $F_s(1)$ increases with increasing l. The further addition of each step element changes the free energy by a constant amount

$$\epsilon = ab(2\sigma_e - l\Delta f) \quad (4)$$

The energy decreases as long as the energetic cost of forming a fold is surpassed by the interaction energy of the new strand with the growing crystal. This condition is satisfied as long as $l > 2\sigma_e/\Delta f$, and the larger the value of l, the faster the free energy decreases with further growth. As a new strand is added, the volume of the two dimensional embryo is increased with no increase in lateral surface. This is true for the transition from $\nu = 1$ to $\nu = 2$, as well as all subsequent additions. Thus, the maximum in the free energy occurs for $\nu = 1$ (ref 19). The value of l corresponding to those folds which most rapidly nucleate and become stable will be the most likely to occur[33].

According to Hoffman[19] the free energy of activation for nucleating the first segment onto the growth face can be given alternatively as

$$\Delta F_a = bl(2\sigma - \Psi a\Delta f) \quad (5)$$

This expression differs from ΔF_s (1) by the introduction of a parameter Ψ, which is concerned with the path by which the first step element of the surface nucleus is attached to the surface. It has been postulated that crystallizing polymer molecules are initially physically adsorbed onto the crystal surfaces[19]. A polymer molecule in the undercooled melt or solution diffuses to the surface of the crystal and is adsorbed onto it. Then, by surface migrations and rotations, the molecule can eventually come to a crystallization site.

If the polymer molecule proceeded directly from the solution or subcooled melt onto the surface at the crystallization site without an intervening adsorption state, such that each segment simultaneously acquired its lateral surfaces and free energy of fusion, then Ψ has a value of 1.0 and in the expressions for the free energy of activation, $\Delta F_a = \Delta F_s$ (1). Values of Ψ less than unity correspond to cases where the polymer molecule is physically adsorbed onto the surface prior to crystallographic attachment. The adsorbed polymer molecule will resemble a two dimensional random coil and will maintain several contacts with the surface of the crystal[34–38]. The fractional coverage of the adsorbed layer can range from 10 to 50%, and can block the deposition of whole step elements directly from the melt (as for $\Psi = 1$). On the other hand, 'loops' (segments between contacts on the surface) can in places become extended enough to produce regions where a lateral surface free energy is expended without involving any corresponding free energy of fusion. Polymer segments in this condition lead to Ψ values less than unity[19].

Both the conditions $\Psi = 1$ and $\Psi = 0$ are regarded as extremes, and it is expected in real polymers that $0 < \Psi < 1$[19]. The sequence of events involved in polymer crystallization is therefore diffusion to the surface → surface attachment → surface migration → crystallographic attachment.

COMPUTATIONAL METHOD

The computer programs used here have been described previously[40]. The approach utilizes a grid-search technique to determine molecular packing parameters to the desired accuracy. The molecules were allowed three dimensional translational freedom. Rotation of the molecules about their chain axes was also allowed. In all cases, the molecules were held internally rigid and parallel to one another and to the growth plane. The increments used in this investigation were as follows: 1° steps for rotation, 0.20 c for shifts parallel to the molecular axis, and 0.01 a and 0.01 b for shifts in the a and b cell directions. The position of a molecule was designated by the fractional co-ordinates, f_a and f_b, of the point of intersection of its axis with the ab plane of the unit cell. The individual molecules were held rigid in the planar zigzag conformation with parameters as follows: C–C–C bond angle 112.0°; H–C–H bond angle, 109.4°, C–C bond length, 1.534 Å, and C–H bond length, 1.090 Å.

The steric potentials used were those in set I of ref 39. These potential functions have been extensively used in calculations on hydrocarbons and give quite reasonable results[1,3,4–7]. It should be noted however that the calculated energies do not correspond directly to the free energy.

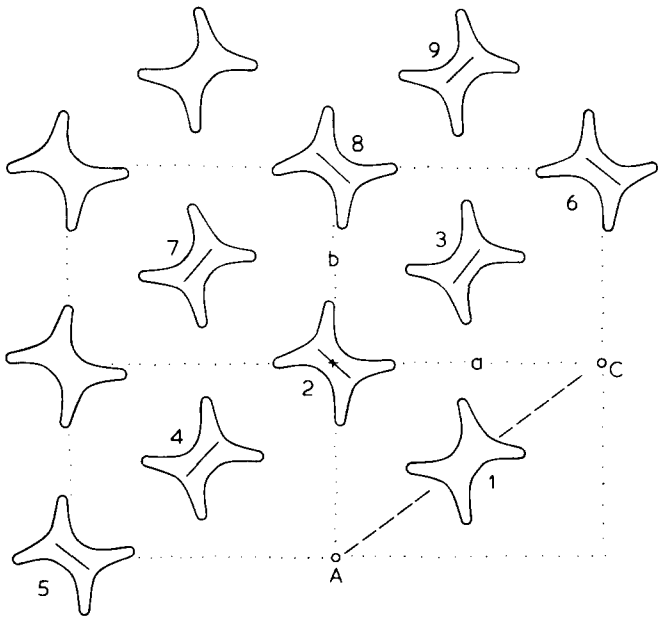

Figure 1 Schematic illustration of the model {110} crystal sector. Chain 1 was moved between positions A and C. The origin is indicated by *

Thermal energy is only approximated and entropic effects are not taken into account.

The values used for a and b dimensions and setting angle of the zigzag plane of the backbone with respect to the b axis for the orthorhombic crystal structure of polyethylene were 7.25 Å, 4.95 Å, and 47° respectively[4]. These values correspond to the lowest energy for the orthorhombic packing geometry of polyethylene chains. While it might have been preferable to calculate using experimental cell parameters near the crystallization temperature, minimization calculations performed on a system artificially constrained at other than minimum energy conditions are subject to substantial errors, analogous to looking for a local minimum on an energetic hillside! The crystal parameters used here were comparable to values observed for orthorhombic n—paraffins and polyethylene in the temperature range of the data from which the potentials were derived[41, 42].

The chain segments used in the calculations were eight methylene units long. It has been estimated that this length represents the molecular segment which could be expected to act (semi-) independently of the rest of a polymer molecule[4]. Aside from the obvious computational reduction, use of a relatively short chain length is necessitated by the assumption of geometrically rigid chains. Energy values reported here will be based on this eight methylene chain fragment to which the term 'segment' refers.

The packing energies were calculated for the interactions between a given chain and at least eight closest neighbours (chains 2 to 9) as shown in *Figure 1*, a schematic illustration of the model {110} crystal sector for the orthorhombic packing geometry of polyethylene chains. About 93% of the total energy contributions to chain segment 1 comes from its interactions with its first three neighbours (chains 2, 3, 4). Chains 2, 3, 4 contribute 56%, 32% and 5%, respectively, of the total interaction energy. The remaining five neighbours contribute only 7% to the total interaction energy: yet more distant interactions would have a much smaller effect and have therefore not been considered.

Structure of the {110} Growth Face

Implicit in theoretical treatments of polymer crystallization has been the assumption that the molecules in the growth face of the crystal have essentially the same positions as they would have if imbedded within the crystal[2]. While this is certainly a necessary and probably reasonable assumption, it has not been investigated before. Energetics calculation offers a straightforward approach to examine the question. The general computational approach was to attach the first segment on the growth face in its energetically most favourable disposition. Then its first two neighbours (for the {110} growth face, at the distances approximately 0.5 $(a^2 + b^2)^{1/2} = 4.39$ Å) were brought in sequentially and allowed to attain their energetically most favourable dispositions. With its two neighbours held rigid on the growth face, the first segment was allowed to relax its position and rotation until it re-attained its most favourable disposition. Each of the neighbours were also allowed to relax (with their corresponding two neighbours on the growth face present) until they also attained their minimum energy dispositions. These procedures were repeated along the growth face until the repetitive pattern along the growth face was established. The substrate, upon which the growth face was built, was assumed to have the same structure as it would have if imbedded within the crystal.

In order to build the {110} growth face, chain segment 1 (*Figure 1*) was brought onto the {110} growth face. The minimum energy disposition for this segment corresponds to $f_a = 0.51, f_b = -0.49$ and setting angle $\theta = 47°$. (The determination of this minimum energy disposition included calculating the energy values for chain translations parallel to the c unit cell direction. As expected, an identical energy minimum was observed after 180° chain rotation and 0.5 c translation). This disposition differed very little from the corresponding crystallographic position $f_a = 0.50, f_b = -0.50$, $\theta = 47°$. The energy of interaction for this eight methylene chain with the crystal was -7.5 kcal mol^{-1}. Chain 10 was then brought onto the growth face. The minimum energy disposition for chain 10 was $f_a = 1.00, f_b = 0.01$ and $\theta = 133°$. The corresponding energy released for this process was 11.7 kcal mol^{-1}. Holding chains 1 and 10 rigid, chain 11 was then brought in. Its most favourable disposition was $f_a = 0.0, f_b = -0.99$ and $\theta = 133°$. Energy released for this process was also 11.7 kcal mol^{-1}, since chains 10 and 11 are crystallographically equivalent. Chains 10 and 11 were then held rigid and chain 1 was allowed to relax. The optimum disposition for chain 1 did not change. Its total interaction energy, including its two neighbours on the growth face, was -16.0 kcal mol^{-1}. Then, chain 11 was allowed to relax with its two neighbours present on the growth face. These two neighbours were chain 1 and its equivalent on the other side of chain 11 at $f_a = -0.49, f_b = -1.49, \theta = 47°$. The most favourable disposition for chain 11 remained $f_a = 0.0, f_b = -0.99$ and $\theta = 133°$. The energy of interaction was also the same as that for chain 1, that is -16.0 kcal mol^{-1}. It seemed therefore that the dispositions of chains 1 and 11 (or 10) provide the repetitive structural pattern along the growth face. The structure of the {110} growth face with chain segment 1 as the nucleating segment is shown in *Figure 2*. This structure is about the same as that found imbedded within the crystal. A total of 31.0 kcal mol^{-1} was released when this secondary nucleus (containing segments 1, 10 and 11) was built. Starting with this structure of the {110} growth face as the substrate, one more {110} growth face was built, with similar chain dispositions observed and the

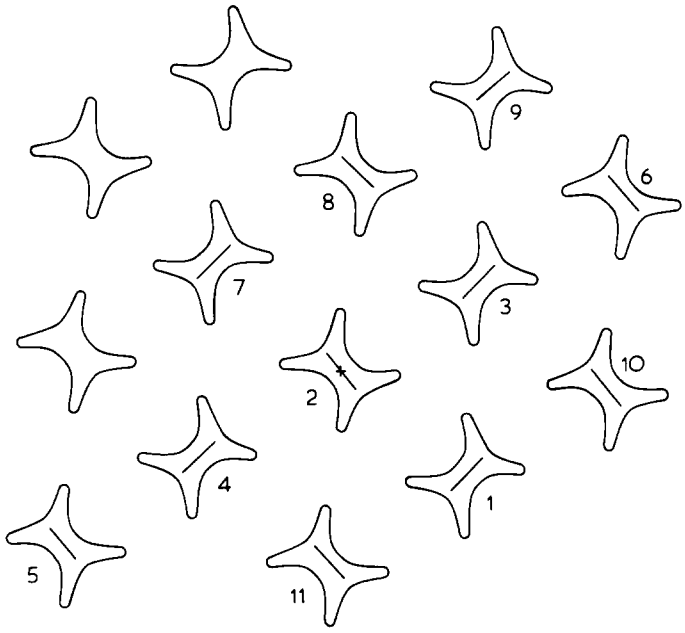

Figure 2 Structure of the {110} growth face with chain 1 as the nucleating segment. The origin is indicated by *

same amount of energy (31.0 kcal mol^{-1}) released.

The structure of the {110} growth face was quite different when the first segment was attached at the low energy position near $f_a = 1.0, f_b = 0.0$. *Figure 3* shows the structure of the {110} face when built with chain 10 as the nucleating segment. The computational procedure was identical to that described previously. The most favourable disposition for the nucleating segment (chain 10), was $f_a = 0.95, f_b = 0.01$ and $\theta = 215°$, compared to the corresponding crystal position, $f_a = 1.00, f_b = 0.00$ and $\theta = +133°$. The determination of this minimum energy disposition included calculations for translations of chain 10 parallel to the c unit cell direction. The minimum energy disposition of the segment was such that the C–C plane was more or less parallel to the growth face ($\theta = 215°$), whereas in the corresponding crystal position, the C–C plane would be approximately perpendicular ($\theta = 133°$) to the {110} growth face. The energy of crystallization in this case ($E = -8.3$ kcal mol^{-1}) was higher than in the previous case with the segment positioned at $f_a = 0.50, f_b = -0.50, \theta = 47°$ ($E = -7.5$ kcal mol^{-1}). Holding chain 10 rigid, chain 12 was brought onto the crystal and its minimum energy disposition corresponded to $f_a = 1.52, f_b = 0.53$ and $\theta = 47°$ and the energy released was 10.5 kcal mol^{-1}. The orientation of chain 12 ($\theta = 47°$) was the same as that dictated by the crystal structure ($\theta = 47°$) but the position was slightly different, the corresponding crystallographic position being $f_a = 1.50$ and $f_b = 0.50$. Energy released in forming this two-chain nucleus is 18.8 kcal mol^{-1}. The corresponding energy released for the two-chain nucleus in the crystallographic positions was 19.2 kcal mol^{-1}, suggesting that there could be a reorientation of chain 10 to allow it to assume its crystal position. Holding chains 10 and 12 fixed, chain 1 was brought onto the crystal face and its minimum energy disposition was $f_a = 0.49, f_b = -0.57$ and $\theta = 133°$ ($E = -10.9$ kcal mol^{-1}). The orientation for chain 1 ($\theta = 133°$) was also quite different from that dictated by the crystal structure ($\theta = +47°$). (It should be noted that a two-chain nucleus consisting of segments 1 and 10 had the same energy as a nucleus having a crystallographic structure.) Finally, chain segment 10 was relaxed with its two neighbours (chain 12 and chain 1) present and the new minimum energy position acquired by the chain was $f_a = 0.96, f_b = 0.01$ and $\theta = 227°$. This disposition was still more or less parallel to the growth face. Three additional chains were added to the crystal face without establishing any repetitive pattern along the face.

The structure of the {110} growth face can be quite different from that dictated by the crystal structure. The total energy released in forming the secondary nucleus containing chains 10, 12 and 1 was 29.6 kcal mol^{-1}. The corresponding energy released for forming the type of nucleus in *Figure 2*, where the chains were more or less in the positions dictated by the crystal structure, was 31.0 kcal mol^{-1}. Thus, by the time the three chains were added to the crystal face in *Figure 3* there was some motivation for these chains to reorient themselves; although, allowed to move individually, segment 10, for example, did not achieve a lower energy in its crystallographic position. Subsequent crystal structure dictates that these chains do come to their crystal positions eventually, but how and when they will do so is not clear. There are two possibilities by which this might occur. One possibility is that some co-operative movement takes place among these chains, since there is some energy advantage in doing so. The other is that a nucleus is not formed by a one-by-one, sequential process, but instead there is some degree of interchain co-operative movement in the adsorbed layer, allowing several segments to crystallize almost simultaneously to form the nucleus. The first alternative requires some kind of co-operative movement among the crystallized segments; whereas the second requires the same co-operation among the physically adsorbed segments. The second alternative may be a more likely process, qualitatively, since the mobility required for co-operative movement will be more readily available among the physically adsorbed segments.

In highly concentrated solution and melt of polymers, the presence of a folded bundle-like structure (as opposed to a coiled polymer molecular structure) has been postulated[44]. The concept of simultaneous nucleation would be supported

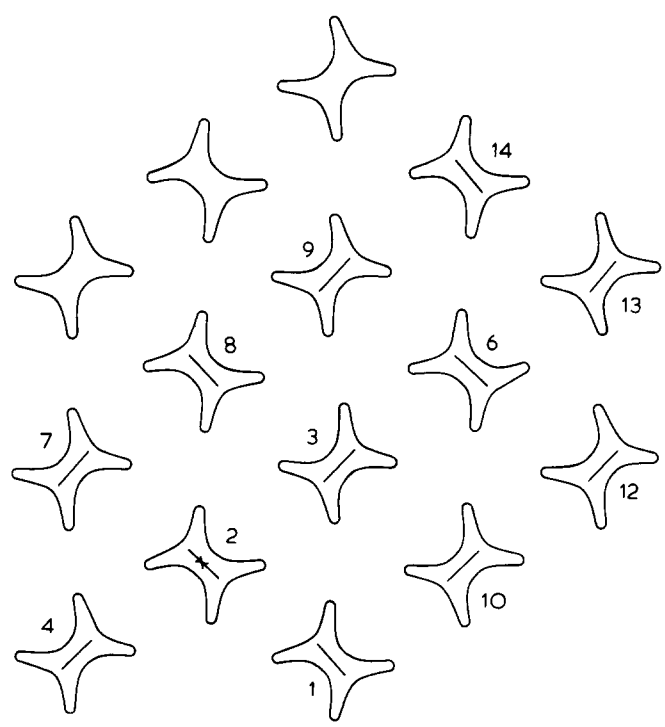

Figure 3 Structure of the {110} growth face with chain 10 as the first nucleating segment. The origin is indicated by *

by the presence of such structures. However, simultaneous nucleation, as presently suggested, could occur either directly from the solution or melt or via co-operative movement among the adsorbed polymer segments which may or may not have bundle-like structures.

Chain mobility on the {110} growth face

The mobility of molecular segments on a growth face may play a significant role in polymer crystal growth, bringing kinetic factors into the crystallization process in addition to their role in the determination of lamellar thickness[19]. While the relative energies for attaching the first molecular strand would be expected to determine (thermodynamically) the frequency of nucleation on the different available growth faces, kinetic factors associated with chain mobility will play a role in the subsequent growth of these nuclei. Mobility should be especially important, for example, after the initial attachment of a molecule onto a growth face upon which growth has previously commenced at some other (distant) location. Mobility may also play some role in determining the mechanism whereby (i) an adsorbed molecule (in its nearly two-dimensional coiled state) rearranges itself to give an extended molecular strand (secondary nucleus) on the growth face, and (ii) the adsorbed molecule presents additional strands to build that nucleus to a stable and viable size. Present concepts of spherulitic growth involving two growth regimes[19] (differing in the relative rates of growth and initiation), may be a reflection of this interplay between thermodynamic and kinetic factors. For crystallization preceeded by adsorption, the rate of chain migration on the crystal faces (lateral and fold) must contribute significantly to the growth rate, while the rate of initiation (secondary nucleation) may depend more upon the energetics for one strand settling onto the growth face.

In the case of single crystal growth, where the rate of secondary nucleation is the controlling factor, one also anticipates some effect of surface migration rates on the relative amounts of different sectors formed. While the initial nucleation event will be most likely to occur on the surface where the energy for the first attached molecular strand is lowest, the lateral spreading rate will be higher and a nucleus will become stable more rapidly on the growth face where the barriers to surface migration are lowest. This is the case because the first segment nucleating on the growth surface requires several neighbours before it can become stable. This coalescence of several strands most likely involves some degree of surface migration (as described above), either to draw additional segments of the same (adsorbed) molecule into the nucleus, or to bring segments of a new incoming molecule to the growth niche. The probability of a new, incoming, molecule associating with the growth face precisely at the active growth niche must be rather low and a matter of chance. Relatively facile surface mobility would enhance the crystallization rate by allowing a molecule to attach to the growth face at any point and then to diffuse to the active growth site. On a surface with relatively high barriers to mobility, on the other hand, attachment of new molecules would have to occur fairly near to the growth site if crystallization were to occur rapidly.

By placing a molecular segment in the vicinity of a growth face at various positions along the face and at various distances from that face, and by calculating the segment's interaction energy with the surface, energy contour maps were obtained which describe the energy field near the surface. From these, estimates of the energy barriers to migration on or near the surface were determined. The contour maps also allowed a qualitative assessment of whether a molecular segment could indeed move on the surface, or whether some degree of disassociation would be required for lateral movement on the growth face. Obviously, it was necessary to make some preliminary assumptions about the structure of the growth face. Again it was assumed that the growth face of the crystal had essentially the same structure as it would have if imbedded within the crystal – that is, the molecules were at their crystallographic positions. The results of the investigation of the structure of the {110} polyethylene crystal growth face indicate that this assumption was reasonable. It was found, not surprisingly, that a molecular segment placed on the surface at its crystallographic position and orientation achieved its minimum energy at a distance (from the growth face) which placed it on the next {110} crystallographic plane. Movement in this plane then will hereafter be referred to as movement 'on the growth face'. It should also be pointed out that movement of the molecule closer to the growth face gave a very rapid increase in energy, such that a plot of interaction energy *versus* distance from the surface takes on the typical appearance of '6–12 potential' curve.

In order to determine the energy field in the vicinity of a {110} growth face, the chain was moved along the {110} growth face such that the increment in the a cell direction was $0.1a$. In addition, at each point on the growth face the chain was rotated through 360° in 10° increments. The chain was moved from the fractional positions 0.0, 1.0 (f_a, f_b) to 1.0, 0.0 with chain 2 taken as the origin in the model shown in *Figure 1*. *Figure 4a* is the energy contour map for these positions and rotations along the {110} growth face. Positions on the growth face are given as fractional a coordinates. The corresponding b coordinate will be $f_b = f_a - 1.0$. Rotations were performed in the clockwise direction from the starting value of the setting angle equal to 47°. The possible crystallographic positions of the segment then would correspond to the position $f_a = 0.5$ and a rotation of 0°, or $f_a = 1.0$ (or 0.0) and a rotation of 86°.

The effect of moving a chain segment parallel to the {110} growth face but 0.30Å and 0.60Å away from the face in the normal direction were also studied. *Figures 4b* and *4c* show the energy maps obtained for different positions and rotations along these planes parallel to the {110} face. Various chain positions in these figures are relative to the fractional a coordinates before the step in the normal direction was taken. For example, in *Figure 4b*, which corresponds to the plane parallel to the growth face but 0.30Å away from it, the position $f_a = 0.5$ corresponds to the position on the growth face before the step in the normal direction was taken, so that actual coordinates of the chain in this case would be $f_a = 0.524$, $f_b = -0.55$.

It is worthwhile considering some of the qualitative or semiquantitative information contained in *Figure 4a*. Vertical sections taken through the map represent the energy values corresponding to different rotations at a given position on the growth face. The positions for which these energy values are low and similar will offer more rotational freedom (and thereby higher rotational entropy) than those positions whose rotational energy values differ widely. For cases where the calculated energies are comparable, the higher entropy will contribute to a lower activation free energy for the nucleation process, making such positions more attractive to a nucleating segment. For example, the energy profiles at growth-face positions 0.2 and 0.4 entail much higher energy peaks than the profiles at 0.0 or 0.5, the crystallo-

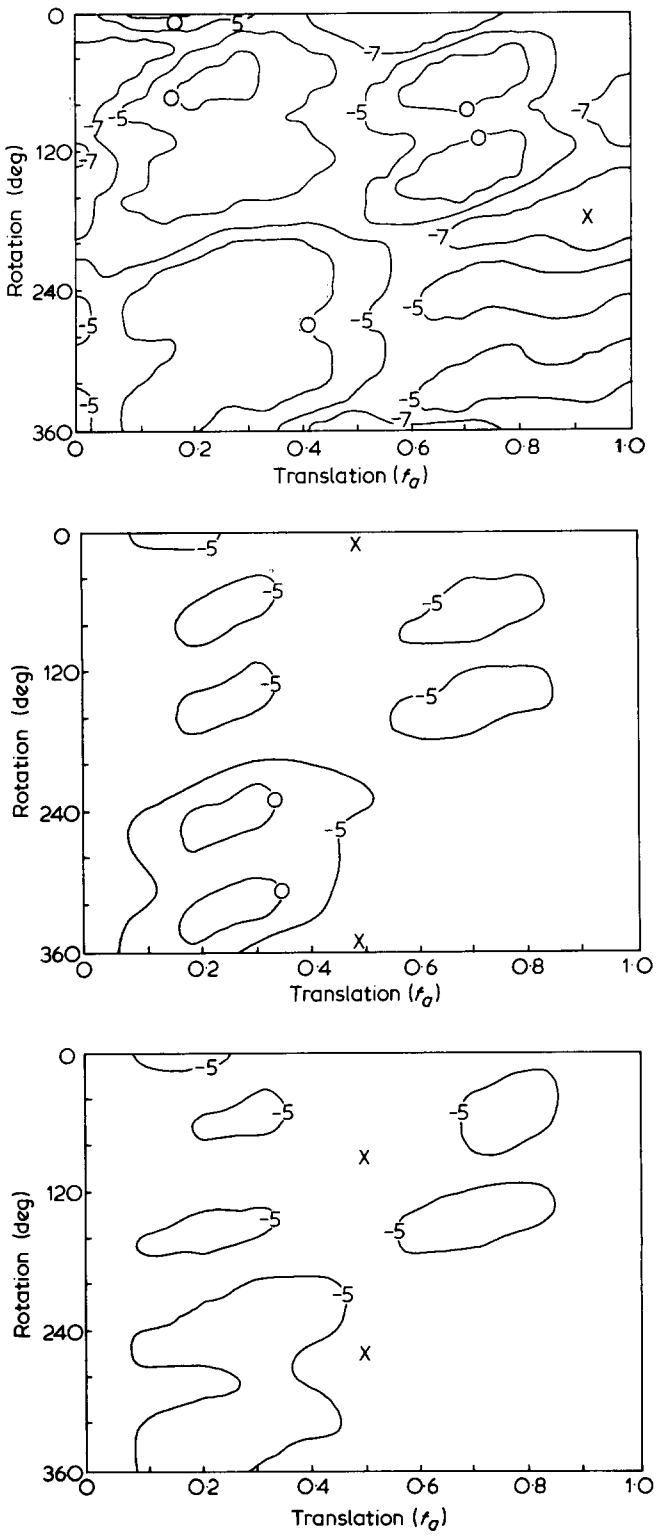

Figure 4 Energy contour maps for rotation and translation on the {110} growth face (a), on a plane 0.30Å away from the face (b), and on a plane 0.60Å away from the face (c). The position of lowest energy is designated by the symbol x. Energies are representative for an eight-methylene chain segment and contours are drawn at 2 kcal mol^{-1} intervals

graphic positions. The positions at 0.6, 0.7, 0.8 are also lower in rotational entropy than the crystal positions.

The minimum energy values for different f_a positions on the growth face are plotted in *Figure 5*. The energy profile is relatively flat, particularly for positions between $f_a = 0.5$ and 1.0, and shows only local energy minima at the crystallographic positions. This indicates that there is little or no energy benefit involved in nucleating at the crystallographic positions compared to noncrystallographic positions. Since it is not possible to evaluate reliably the entropy considerations mentioned above, it is not clear whether the entropic advantages offered by the crystallographic positions would be sufficient to direct the first chain segment to these sites preferentially. It can be concluded, however, that nucleation at crystallographic sites would not occur exclusively.

Comparison of *Figures 4b* and *4c* with *4a* indicate that the positional freedom of a chain segment has increased considerably. This is expected, since, as the chain is progressively moved away, it becomes less responsive to the restrictions imposed by the crystal. However, it is noted that the steps taken in the normal direction are small and the segment is still attracted to the crystal (as indicated by the predominance of low energy values in the map). The energy differences between the various low energy dispositions are smaller than those for a molecule on the growth face.

Examination of the energy surface depicted in *Figure 4a* indicates that the two distinct low energy regions of the map (recalling that the map will be periodic and the surface represented will be duplicated along each edge) are separated by an energy barrier of 2.5 kcal mol^{-1} for a segment moving from $f_a = -0.05$ to $f_a = 0.5$ and by a barrier of 1.6 kcal mol^{-1} for motion from $f_a = 0.5$ to $f_a = 0.95$. When a molecular segment undergoes this same lateral motion on a plane 0.30Å away from the growth face (*Figure 4b*), the barriers to these same positional shifts are both about 0.5 kcal mol^{-1}. However, 1.2 kcal mol^{-1} is required to move the segment away from the face by 0.30Å. Similarly, for a plane 0.60Å from the growth face, as indicated in *Figure 4c*, virtually the entire surface is accessible at little cost in energy; but removing the segment from the surface requires about 2.0 kcal mol^{-1} From these results, it appears that even a molecular segment on the growth face would not encounter large barriers to lateral diffusion. While some advantage may be gained by a slight shift away from the growth face, the energetic cost of a shift greater than about 0.30Å would probably outweigh any gain in the lateral diffusional energetics.

The surface migration of physically adsorbed molecules is thought to bring chains from the site of their initial attachment into their eventual crystal positions[20]. The physically adsorbed molecule will have different segments at varying distances from the growth face. The relative mobility of an adsorbed molecule is clearly most strongly influenced by the segments on or near the growth face. Segments removed far enough from the growth face (weakly adsorbed segments) will be very mobile, no matter what type the growth face. These calculations for the {110} growth face indicate that even those segments on the growth face are quite mobile.

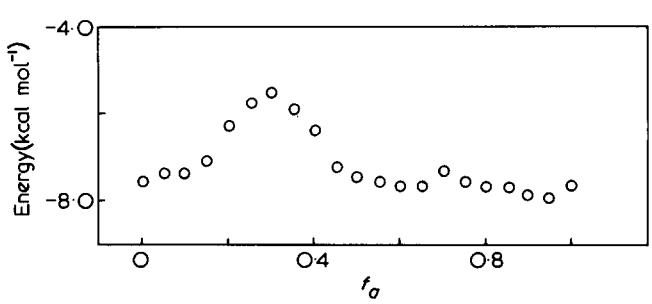

Figure 5 Energy *versus* chain position on the {110} growth face. The energy values correspond to the lowest energy rotational orientation of the molecule

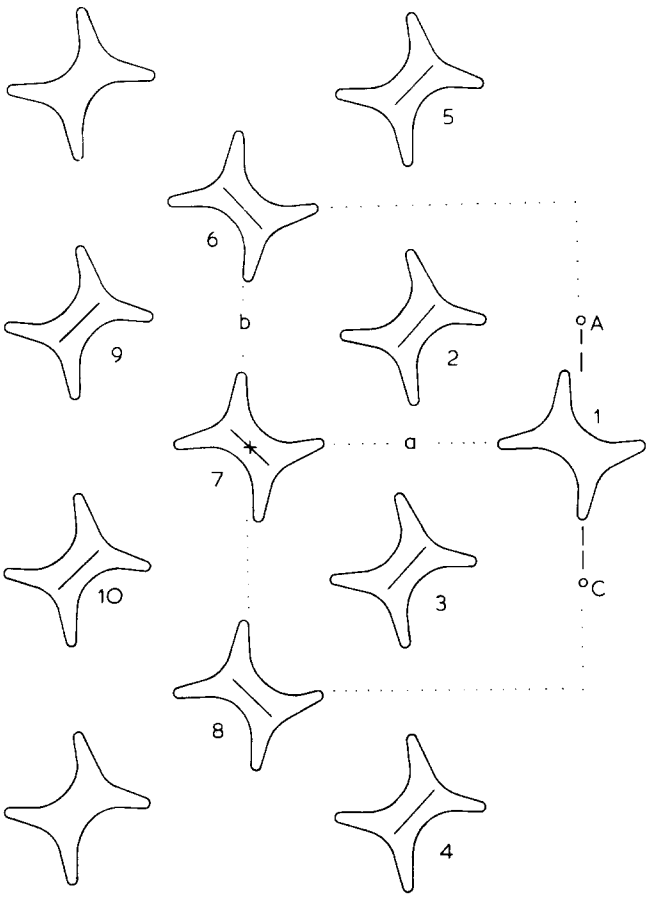

Figure 6 Schematic illustration of the model {200} crystal sector. Chain 1 was moved between positions A and C. The origin is indicated by *

Chain mobility on the {200} Growth face

The computational procedure followed for examining the {200} face was identical to that followed for {110} face, and the model is shown in *Figure 6*. *Figures 7a, 7b* and *7c* show the energetics data on the {200} growth face and on parallel planes 0.36Å and 0.72Å away in the normal direction, respectively.

The position on the growth face is designated by the f_b coordinate of the segment. Rotations were performed in a clockwise fashion from the starting value corresponding to the crystallographic setting angle for the chain segment. Thus, the crystallographic position for the chain is located at the $f_b = 0, \theta = 0^\circ$ position on the energy map.

Figure 7a displays the energy contour map for various positions and rotations along the {200} growth face. As in the previous figures, vertical sections taken through the map represent energy values corresponding to different rotations at a given position on the growth face, and provide some qualitative information about the rotational entropies involved. From the data in *Figure 7a*, a chain segment at the crystal position ($f_b = 0.0$) has greater rotational freedom than it would at the noncrystallographic positions, although, in general, the {200} face offers less rotational freedom to nucleating segments than the {110} face. Also, the examination of low energy dispositions of the chain at various f_a positions on the {200} growth face reveals (*Figure 8*) an absolute energy minimum at the crystal position ($f_b = 0.0$). The energy increases rather sharply as the chain is moved away from the crystal position into noncrystallographic positions. Therefore, for the first segment nucleating on the {200} growth face, there seem to be energetic as well as entropic benefits involved in nucleating at the crystal position. This is in sharp contrast with the {110} face, which offered only local energy minima at the crystal positions and about the same energy for a nucleating segment at any of the non-crystallographic positions between $f_a = 0.50$ to $f_a = 1.0$. The features of the {200} and {110} growth faces which give rise to this substantial difference in the energy maps can

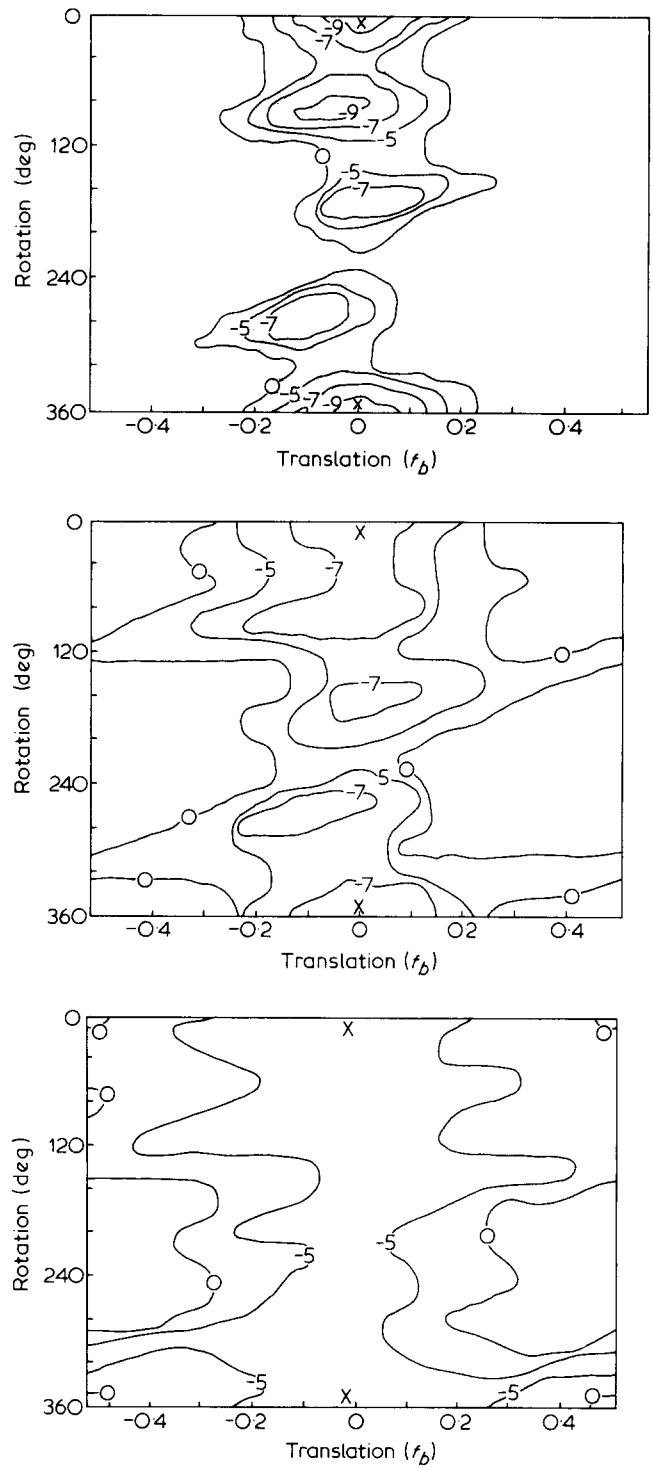

Figure 7 Energy contour maps for rotation and translation on the {200} growth face (a), on a plane 0.36Å away from the face (b), and on a plane 0.72Å away from the face (c). The position of lowest energy is designated by the symbol x. Energies are representative for an eight methylene chain segment and contours are drawn at 2 kcal mol^{-1} intervals

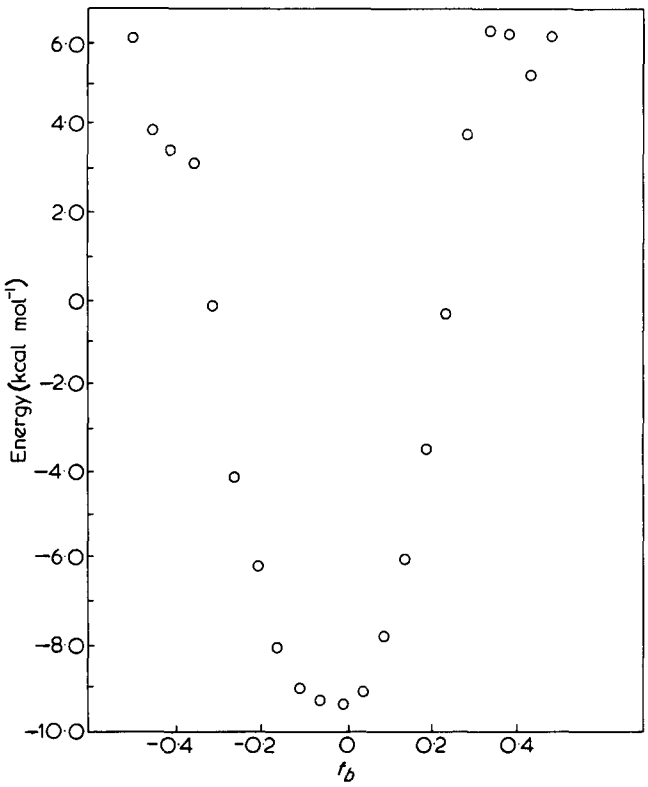

Figure 8 Energy *versus* chain position on the {200} growth face. The energy values correspond to the lowest energy rotational orientation of the molecule

be seen by comparing *Figures 1* and *6*. The {110} growth face presents a fairly even surface to an incoming chain segment, while the {200} face has fairly well-defined grooves between adjacent chains in the growth face (e.g. between chains 2 and 3 in *Figure 6*). Essentially an incoming segment on the {200} face nestles into this groove in coming to its lowest energy disposition. Subsequent movement in the plane at this distance (0.5*a*) from the growth face rapidly leads to severe steric interactions with the protuberant hydrogen atoms from the polyethylene chains constituting the growth face. Thus, once having assumed a position 'on the growth face', the chain segment is effectively prevented from lateral motion on the face.

It should be noted in passing that there is a low energy disposition for the first nucleating segment on the face where the molecule is rotated about 90° from the crystallographic setting angle and shifts slightly from the crystallographic f_a and f_b position. The energy for a segment at this position was only slightly (less than 0.1 kcal mol^{-1}) higher in energy than the crystal disposition. Using a molecule in this position as the first segment on the face, neighbouring chains were brought into their lowest energy positions on the face. As on the {110} face, the nucleus formed by placing segments in such low energy noncrystallographic dispositions had a higher overall energy than a nucleus having all chains in their crystallographic positions.

Figures 7b and *7c* show the energy maps for moving a chain segment on the planes parallel to the {200} growth face but 0.36Å and 0.72Å away in the normal direction, respectively. The energy barriers for chain mobility on both of these planes remain more severe than in their counterparts for the {110} face. Even on the plane 0.72Å away from the growth face, the lateral movement on the face (say from f_b = 0.0 to f_b = 1.0) involves an energy barrier of about 2.0 kcal mol^{-1}. The energetic cost in removing the segment from the growth face to this plane is about 3.0 kcal mol^{-1}. Thus, while modest detachment of the segment lowers the energy barrier to lateral motion to moderate values, the barrier remains substantially higher than those on the {110} face.

It is noted that substantially more energy is gained by a chain nucleating on the {200} growth face (E = −9.5 kcal mol^{-1}) than by a chain nucleating on the {110} growth face (E = −7.5 kcal mol^{-1}). Assuming that the changes in entropy involved in going from solution or melt to either the {110} or {200} growth face are equal, there is a lower free energy of activation involved for nucleation on the {200} growth face than on the {110} face. For successful nucleation, however, the nucleus must grow to the stable size where ΔF becomes negative. Higher surface mobility can be expected to give a higher lateral spreading rate and allow the nucleus to grow to this stable size more rapidly. Thus, although a chain can nucleate faster on the {200} face, redissolution or reversion to an adsorbed coil may be its more likely prospect: it cannot grow to a stable size as quickly as could a nucleus on the {110} face. Because of the relative ease of chain mobility on the {110} face, the {110} growth face may have a kinetic advantage over the {200} face, although this may not be sufficient to override the {200} face advantage of nucleation energetics.

Entropies of growth surfaces

In that the entropy contribution to the free energy for a molecular segment is a measure of its positional freedom on the surface, a qualitative estimate for the entropy differences on the {110} and {200} growth faces can be determined by inspecting the energy contour maps shown in *Figures 4* and *7*. The greater expanses of the low energy areas on the maps for {110} surface correspond to greater positional freedom than is found for the {200} face where the low energy regions are more localized. This visual impression of different energy surfaces can be put onto a semiquantitative basis. The positional freedom of a segment on the surface should be reflected in a measure of the 'accessible regions' of the energy contour map – which should in turn be related to the total 'volume' of the energy surface. That this might be the case can be seen by considering two low energy regions of comparable minimum energy, one a rather steep-walled energy well and the other a substantially broader well[45]. It would be expected that the broad well would encompass more energetically accessible states in the vicinity of the minimum, and would therefore have higher entropy than the steep well.

In the present case, since the energy maps cover the same ranges of the variables (rotation and translation on the surface), a calculation of the volumes of the entire energy surfaces should yield values related to their respective entropies. The volume of each surface has been determined by approximating the energy surface by rectangular parallelepipeds having two dimensions (a 20° rotation edge and a 0.10 fractional position edge) constant, with the third dimension the energy/length of the block, measured from the energy surface to the 0.0 kcal mol^{-1} level. Operationally then, because two dimensions of the blocks are constant during the summation, this 'area' term will provide only a constant multiplicative factor. A measure of the relative volumes of the surfaces, therefore, can be determined merely by summing up the negative energy values in the map. While the actual values computed have little meaning, the relative values comparing the

two surfaces should be significant. The ratios of the {110} entropy to the {200} entropy were 3.1, 2.2 and 1.6 for segments on the growth face, 0.30Å removed and 0.60Å removed, respectively. The corresponding ratios of the numbers of volume elements in the negative-energy regions of the maps were 3.2, 1.7 and 1.2. These results clearly indicate that the entropy for a molecular segment on the {110} face is considerable greater than that on the {200} face, but that the entropic advantage of the {110} face decreases with increasing distance from the surface. (Although the contour maps for the {110} and {200} surfaces encompass the same range of the variables – namely 360° of rotational variation and fractional coordinates from 0.0 to 1.0 (or −0.5 to 0.5) – there was a small correction to be applied to the calculated entropy values. This correction was required because the distance covered by a molecule moving from 0.0 to 1.0 f_a on the {110} face is 4.39Å, while the corresponding distance on the {200} face is 4.95Å. To put the values on an equal area basis, this 11% correction was applied to the calculated entropy ratios). The major changes in the energy maps that give this progression of values take place predominantly in the {200} map, as can be seen by comparing *Figures 4* and *7*. For a chain segment on this growth face, only 27% of the map has negative energy values, while this portion increases to 55% and 81% for a segment 0.3Å and 0.6Å away, respectively. On the {110} face the corresponding negative energy regions constitute 84%, 95% and 100% of the contour maps.

The greater entropy of the {110} face will decrease the difference in activation free energies for nucleation on the {110} and {200} growth faces from the calculated energies presented earlier. Obviously, the results of this qualitative evaluation of entropies of the two surfaces cannot be combined with their respective energies to determine the relative free energies of segments on the growth faces. A more quantitative evaluation of the entropy can be made, however, by calculating the partition function and the average relative energy for each contour map, based upon the same volume-element analysis of the surface described above. Such an analysis yields entropies of 10.6 eu and 7.6 eu for segments on the {110} and {200} surfaces respectively (a ratio of 1.4). Using a crystallization temperature of 370K, this entropy difference could decrease the difference in the free energy for segments on the {200} and {110} faces by about 1.1 kcal mol^{-1} from the energy values resulting from the energetics calculations. This leaves a difference in free energy of about 0.9 kcal mol^{-1} for eight methylene chain segments on the growth faces.

DISCUSSION

Truncated crystals

As noted earlier, polyethylene crystals are normally diamond-shaped, but when prepared at higher crystallization temperatures or from solutions of higher polymer concentration, the crystals develop sectors having {200} faces as well as the usual {110} growth faces. It is also found that the relative amount of {200} growth to {110} growth increases with increasing crystallization temperature and polymer concentration.

It has been suggested that {200} crystal sectors represent a morphological structure nearer to an equilibrium structure than the {110} crystal sector[12]. This inference has followed directly from the increased degree of truncation of single crystals with increasing crystallization temperature and the accompanying increase in chain mobility and ease of approaching equilibrium. If this were so, one would also expect {200} sectors to have a higher melting temperature than {110} sectors. On the contrary, evidence shows that {200} sectors disorder and melt at temperatures where the {110} sectors are stable[17]. It has also been suggested that the concentration dependence of the degree of truncation may reflect a change from equilibrium to kinetic morphological control[12]. It is possible that a better explanation for both temperature and concentration dependence may be provided by an understanding of the relative energetics of nucleation and growth on the {110} and {200} crystal face.

It has been pointed out[47] that, in crystal growth processes for non-polymeric materials, the smaller facets of a multifaceted crystal will be those upon which growth occurs most rapidly and only the slower growing planes will be preserved as faces on the final crystal. For diamond-shaped polyethylene crystals, one could imagine that any minute amount of {200} growth face that might be present during crystallization would rapidly grow and disappear. The effect would be the same – except on a molecular scale – as a truncated crystal undergoing rapid growth on the {200} faces. Essentially, filling in of the blunted tips of the crystal would continue until the familiar diamond shape was attained. Thereafter growth would continue on the {110} surfaces, since they would be the only ones available. One would conclude that the appearance of macroscopic truncation was due to an alteration in the relative growth rates of the two sectors (due to differences in the crystallization conditions). The implications of this situation are that (1) under conditions of growth, truncated crystals must have fairly similar growth rates on both types of growth faces, (ii) the growth rate on the {200} faces is somewhat greater than that on the {110} faces, and (iii) an increasing degree of truncation indicates a relative increase in the {110} growth rate compared to the {200} growth rate.

The principal results of these calculations are (i) the energy of association of the first segment on a growth face is lower on the {200} face (indicating a greater likelihood for nucleation on this face than on the {110} face, and an increased likelihood for such a nucleating molecular strand to remain extended) and (ii) the surface mobility is much greater on the {110} face (allowing those strands that do nucleate new growth layers on this face to become stable nuclei more rapidly than could occur on the {200} face). Whether the lower energy, slower coalescing (stabilizing) nuclei on the {200} face will provide for faster or slower growth than the higher energy, rapidly stabilized nuclei on the {110} face is questionable. Since at low crystallization temperature, the {200} faces are much smaller than the {110} faces (even to the point of being totally absent), one could infer that indeed {200} growth is the faster process, i.e. the lower nucleation energy takes precedence over the surface mobility factor. This is partially substantiated by considering the temperature dependence of the degree of truncation. Because the energy barrier to mobility is greater on the {200} face than on the {100} face, the temperature dependence of the mobility on that face will be greater than that on the {110} face. As the crystallization temperature is increased, then, one would expect the mobility on the {200} face to increase more rapidly than mobility on the {110} face. If chain mobility were indeed the controlling factor, one would expect the growth rate on the {200} face to increase relative to the {110} growth rate with increasing temperature. On the contrary, experimental data show an increased degree of truncation with increasing temperature, indicative of a *slower*

{200} growth rate (relative to {110} growth). If the nucleation energetics were the controlling factor, nucleation on the {110} face would be disfavoured but have a greater temperature dependence than nucleation on the {200} face. With an increase in temperature, then, one would expect enhancement of the {110} growth rate relative to the {200} growth rate, behaviour consistent with the observed dependence of the degree of truncation on crystallization temperature.

The concentration dependence of the degree of truncation can also be rationalized as an interplay between kinetically controlled mobility and thermodynamic stability of the growth nucleus. Clearly, in more concentrated (but still dilute) solutions, transport of polymer to the growing crystal will be more rapid[48]. On the {200} face, where the first extended molecular strand in the new growth layer is somewhat more stable than its counterpart on the {110} surface, the increased transport would probably have a relatively minor effect since the arriving molecules would rapidly be anchored into the grooves of the surface and prevented from migrating to an active growth site. (There could be a slight growth rate enhancement since the increased arrival of molecules at the face would serve to increase the amount of material that did arrive by chance near a growth site and could therefore crystallize rapidly.) On the {110} face on the other hand, material arriving at the surface at any point would have sufficient mobility to migrate easily to an active growth site, thereby increasing the growth rate on that face. Perhaps more important, however, is the fact that an increased amount of mobile polymer on the face would increase the rate of coalescence whereby a stable and viable nucleus is developed. (The rate of this coalescence will be proportionately more critical on the {110} face than on the {200} face because of the lower stability of the first nucleating strand on the {110} growth face.) These two factors would serve to increase the relative rate of {110} growth compared to {200} growth, again consistent with experimental observation.

The energetics calculations for the packing energy for a molecular segment *within* the {110} face give a value of -16.0 kcal mol^{-1} compared to -14.2 kcal mol^{-1} for the {200} face. The principle interactions that are missing (due to the presence of the surface) for a chain in the {110} surface are those with one molecule a distance b away (4.95Å) and with one molecule at $0.5\ (a^2 + b^2)^{1/2}$ (4.39Å). For a molecule within the {200} face, the missing molecular interactions are with two molecules 4.39Å away. Thus a greater portion of the ultimate heat of fusion is missing for a molecule in a {200} face, indicating that there is less cost in removing it from the surface. Therefore, the calculated packing energies provide an explanation for the lower observed melting point for {200} sectors compared to {110} sectors, assuming melting proceeds from the lateral surface inward.

CONCLUSIONS

Energetics analysis has been used to investigate aspects of the growth process for polyethylene single crystals. This investigation has focussed on interactions of a molecular segment with the growth faces and has considered neither the effects of chain folding nor the packing of folds into a fold surface. Nonetheless, the results provide interesting insight into the nature of the molecular processes involved in the association of molecular segments with the growth faces of the crystal. In particular, the important information gleaned from this study is as follows:

(1) the interaction energy of the first nucleating segment on a {200} surface is lower than that for a segment on a {110} surface;

(2) the mobility of a segment on a {200} face is very restricted, while the mobility of a {110} surface is quite substantial;

(3) examination of the observed temperature dependence of the degree of truncation suggests that the controlling factor in relative growths of the {110} and {200} sectors is the lower nucleation energy on the {200} face rather than segmental mobility factors;

(4) the dependence of the degree of truncation of polyethylene single crystals on the concentration of polymer in solution and upon crystallization temperature has been explained in terms of the relative interaction energies and surface mobilities provided by {200} and {110} growth faces;

(5) the energies of molecules within the {200} and {110} growth surfaces indicate that {200} sectors should melt at lower temperatures than {110} sectors, in agreement with experimental observation;

(6) the lowest energy site for molecular attachment on the {200} face is at the crystallographic position and orientation;

(7) on the {110} surface, the crystallographic position and orientation represents a low energy state, but noncrystallographic positions have lower energy for the first segment added to the growth face;

(8) for {110} surfaces nucleated at a crystallographic position, the growth layer assumes very closely the structure it would have if imbedded within the crystal;

(9) for {110} surfaces nucleated by a molecule in its lowest energy disposition, the growth face is quite different from the crystallographic structure. However, after three molecular segments have been added, a cooperative rearrangement of the molecules must occur to bring the three chain nucleus into the now lower-energy crystalline mode of packing.

While the effects of chain folding and the energetics of packing the folds into a fold surface are certainly important factors that may alter somewhat the conclusions drawn from this limited analysis, it should be noted that the calculated differences between the {110} and {200} crystal faces will be an order of magnitude greater than values presented here when extrapolated to a typical lamellar thickness. For example, the difference in nucleation energy for a molecular strand of 100Å length would be on the order of 20 kcal mol^{-1}. Analyses of various fold conformations in {110} and {200} fold sectors give energy differences in the range of only 1–2 kcal mol^{-1} [49–51]. Thus, in light of the other differences in the {110} and {200} growth faces examined here, the role of chain folds in influencing crystal growth sectorization may be less than might have been expected initially.

ACKNOWLEDGEMENT

The authors grateully acknowledge support from the National Science Foundation, Division of Materials Research (Polymers Program Grant DMR77-20604), and a Washington State University Grant-in-Aid.

REFERENCES

1 Boyd, R. H. and Breitling, S. M. *Macromolecules* 1974, **7**, 855
2 Reneker, D. H., Franconi, B. M. and Mazur, J. *J. Appl. Phys.* 1977, **48**, 4032

3 Boyd, R. H. *J. Polym. Sci., Phys. Ed.* 1975, **13**, 2345
4 Farmer, B. L. and Eby, R. K. *J. Appl. Phys.* 1974, **45**, 4229
5 Farmer, B. L. and Eby, R. K. *J. Appl. Phys.* 1975, **46**, 4209
6 Farmer, B. L. and Eby, R. K. *Polymer* 1979, **20**, 363
7 Eby, R. K. and Farmer, B. L. *Polym. Prep., Am. Chem. Soc., Div. Polym. Chem.* 1976, **17**, 131
8 Williams, D. E. *J. Chem. Phys.* 1967, **47**, 4680
9 Bunn, C. W. *Trans. Faraday Soc.* 1939, **35**, 482
10 Bunn, C. W. and Holmes, D. R. *Discuss. Faraday Soc.* 1958, **25**, 95
11 Wunderlich, B. 'Crystals of Linear Macromolecules', American Chemical Society, Washington, D.C. 1973, p 29
12 Schultz, J., 'Polymeric Materials Science', Prentice–Hall, New Jersey, 1974, p 40
13 Keller, A. *Phil. Mag.* 1957, **2**, 117
14 Till, P. H. *J. Polym. Sci.* 1957, **24**, 301
15 Fischer, E. W. *Z. Naturforsch., Teil A* 1957, **12**, 753
16 Kawai, T. and Keller, A. *Phil. Mag.* 1963, **8**, 1753
17 Bassett, D. C., Frank, F. C. and Keller, A. *Nature* 1959, **184**, 810
18 Heber, I. *Kolloid-Z* 1963, **189**, 112
19 Hoffman, J. D., Davis, G. T. and Lauritzen, J. I. in 'Treatise on Solid State Chemistry' (Ed. N. B. Hannay) Plenum Press, New York, 1975, Vol 3, Chap. 7
20 Hoffman, J. D. and Lauritzen, J. I. *J. Res. Nat. Bur. Std., Sect. A.* 1961, **65**, 297
21 Hoffman, J. D. *Soc. Plast. Eng. Trans.* 1964, **4**, 315
22 Lauritzen, J. I. and Hoffman, J. D. *J. Appl. Phys.* 1973, **44**, 4350
23 Lauritzen, J. I. and Hoffman, J. D. *J. Res. Nat. Bur. Std., Sect. A* 1960, **64**, 73
24 Price, F. P. *J. Polym. Sci.* 1960, **42**, 49
25 Frank, F. C. and Tosi, M. *Proc. R. Soc. London, Ser. A* 1961, **263**, 323
26 Gornick, F. and Hoffman, J. D. *Ind. Eng. Chem.* 1966, **58**, 41
27 Lauritzen, J. I. and Passaglia, E. *J. Res. Nat. Bur. Std., Sect. A* 1967, **71**, 261
28 Lauritzen, J. I. and Hoffman, J. D. *J. Chem. Phys.* 1959, **31**, 1680
29 Price, F. P. *J. Chem. Phys.* 1961, **35**, 1884
30 Hoffman, J. D., Lauritzen, J. I., Passaglia, E., Ross, G. S., Frolen, L. J. and Weeks, J. J. *Kolloid-Z* 1969, **231**, 564
31 Turnbull, D. and Cormia, R. L. *J. Chem. Phys.* 1961, **34**, 820
32 Gornick, F., Ross, G. S. and Frolen, L. J. *J. Polym. Sci.* 1967, **C18**, 79
33 Geil, P. H. 'Polymer Single Crystals', Wiley-Interscience, Pennsylvania, 1963
34 Silberberg, A. *J. Chem. Phys.* 1967, **46**, 1105
35 Hoeve, C. A. J., DiMarzio, E. A. and Peyser, P. *J. Chem. Phys.* 1965, **42**, 2558
36 DiMarzio, E. A. and McCrackin, F. L. *J. Chem. Phys.* 1965, **43**, 539
37 DiMarzio, E. A. and Rubin, R. J. *J. Chem. Phys.* 1971, **55**, 4318
38 Stromberg, R. R., Tutas, D. J. and Passaglia, E. *J. Phys. Chem.* 1965, **69**, 3955
39 Williams, D. E. *J. Chem. Phys.* 1967, **47**, 4680
40 Farmer, B. L. Thesis, Department of Macromolecular Science, Case Western Reserve University, 1972
41 Davis, G. T., Eby, R. K. and Colson, J. P. *J. Appl. Phys.* 1970, **41**, 4316
42 Kavesh, S. and Schultz, J. M. *J. Polym. Sci. A-2,* 1970, **8**, 243
43 Martin, G. M. and Passaglia, E. *J. Res. Nat. Bur. Std. Sect. A* 1966, **70**, 221
44 Wunderlich, B. 'Macromolecular Physics', Vol 2, Academic Press, New York, 1976, p 2
45 Hopfinger, A. J. Case Western Reserve University, private communication
46 Kawai, T. and Keller, A. *Phil. Mag.* 1965, **11**, 1165
47 Khoury, F. National Bureau of Standards, private communication
48 Keller, A. and Pedemonte, E. *J. Cryst. Growth* 1973, **18**, 111
49 Petraccone, V., Allegra, G. and Corradini, P. *J. Polym. Sci. C* 1972, **38**, 419
50 Oyama, T., Shiokawa, K. and Ishimaru, T. *J. Macromol. Sci. Phys.* 1973, **8**, 229
51 McMahon, P. E., McCullough, R. L. and Schlegel, A. A. *J. Appl. Phys.* 1967, **38**, 4123